INTEGRAL

Science Operations Centre

Announcement of Opportunity for Observing Proposals (AO-5)

JEM-X Observer's Manual

INT/SDG/05-0248/Dc

Issue 5.0

12 March 2007

Prepared by P. Kretschmar

Authorised by A.N. Parmar

Based on inputs from the JEM-X team, DSRI Copenhagen (PI: S. Brandt)

Table of Contents

1 Introduction

The Joint European Monitor for X-rays (JEM-X) on-board INTEGRAL fulfils three roles:

It provides complementary data at lower energies for the studies of the gamma-ray sources observed by the two main instruments, IBIS and SPI. Normally any gamma-ray source bright enough to be detected by the main instruments will also be bright enough to be rapidly identified with JEM-X. Note, however, that the field of view of JEM-X is significantly smaller than those of IBIS and SPI. Flux changes or spectral variability at the lower energies may provide important elements for the interpretation of the gamma-ray data. In addition, JEM-X has a higher spatial resolution than the γ-ray instruments. This helps with the identification of sources in crowded fields.

During the recurrent scans along the galactic plane JEM-X provides rapid alerts for the emergence of new transients or unusual activity in known sources. These sources may be unobservable by the other instruments on INTEGRAL.

Finally, JEM-X can deliver independent scientific results concerning sources with soft spectra, serendipitously detected in the field of view (FOV) during the normal observations.

JEM-X operates simultaneously with the main gamma-ray instruments IBIS and SPI. It is based on the same principle as the two gamma-ray instruments on INTEGRAL: sky imaging using a coded aperture mask. The performance of JEM-X is summarised in Table 1.

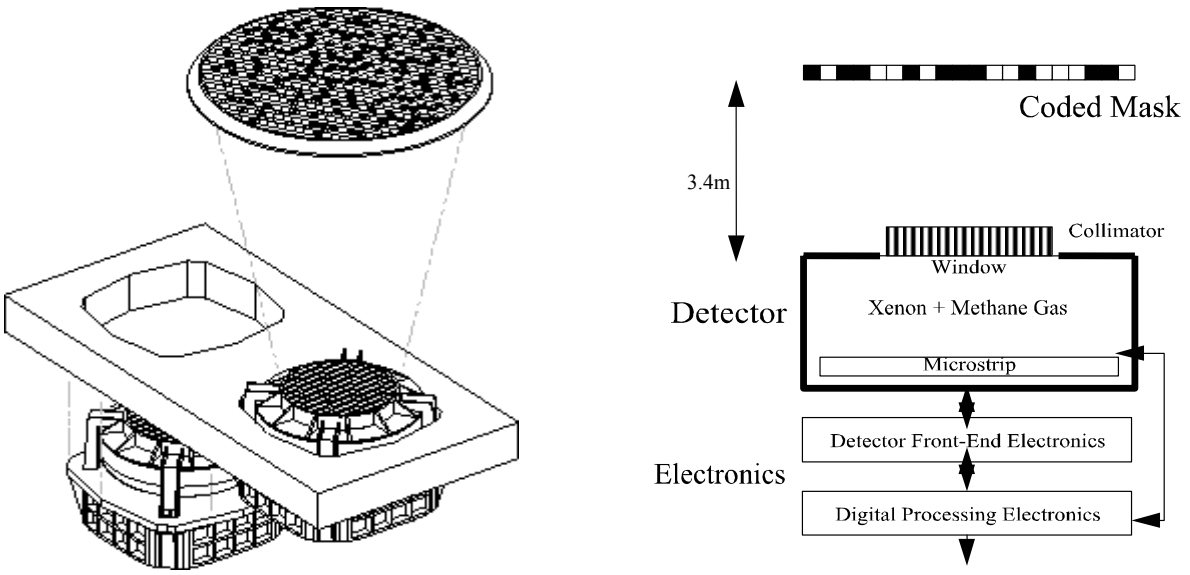

Figure 1: Left: overall design of JEM-X, showing the two units, with only one of the two coded masks. Right: functional diagram of one unit.

Table 1: parameters and performance of the JEM-X1 unit

Parameter	**In-orbit value**
Active mask diameter	535 mm
Active detector diameter	250 mm
Distance from mask to detector entrance window	3401 mm
Energy range	3-35 keV
Energy resolution (FWHM)	$\Delta E/E = 0.40 \times [(1/E\ \text{keV})+(1/40\ \text{keV})]^{1/2}$
Angular resolution (FWHM)	3′
Field of view (diameter)	4.8° Fully illuminated 7.5° Half response* 13.2° Zero response
Relative point source location error	1 ′ (90% confidence radius for a 15σ isolated source)
Continuum sensitivity **for a single JEM-X unit** (isolated source on-axis)	1.2×10^{-4} ph cm^{-2} $s^{-1}keV^{-1}$@ 6 keV 1.0×10^{-4} ph cm^{-2} $s^{-1}keV^{-1}$@ 30 keV for a 3σ cont. detection in 10^5 s, dE = 0.5E
Narrow line sensitivity **for a single JEM-X unit** (isolated source on-axis)	1.6×10^{-4} ph cm^{-2} s^{-1}@ 6 keV 1.3×10^{-4} ph cm^{-2} s^{-1}@ 20 keV for a 3σ line detection in a 10^5 s observation
Timing resolution	122 μs (relative timing) ≈1 ms (absolute timing)

* At this angle the sensitivity is reduced by a factor 2 relative to the on-axis sensitivity. In practice, the transmission of the collimator beyond an off-axis angle of 5° is so low that only the very brightest sources can be observed at larger angles

2 Description of the instrument

2.1 The overall design and status

JEM-X consists of two identical coded-aperture mask telescopes co-aligned with the other instruments on INTEGRAL. In the current configuration the JEM-X "1" unit is operating while JEM-X "2" is dormant. The photon detection system of JEM-X consists of high-pressure imaging Microstrip Gas Chambers located at a distance of 3.4 m from each coded mask. Figure 1 (p. 5) shows a schematic diagram of one JEM-X unit. A single JEM-X unit comprises three major subsystems: the detector, the associated electronics and the coded mask.

At the end of the Instrument Performance Verification phase, it was decided to operate only one JEM-X unit at a time. The switch-off of one of the units was decided after a gradual loss in sensitivity had been observed in both JEM-X units, due to the erosion of the microstrip anodes inside the detector. By lowering the operating voltage, and thereby the gain of the detectors, the anode damage rate has now been reduced to a level where the survival rate of the detectors seems to be assured for the extended mission phase. If in the future both units are to be switched on together again, the total sensitivity will increase by approximately a factor $\sqrt{2}$, however at the time of writing of this document such a change is not being considered.

2.2 The detector

The JEM-X detector is a microstrip gas chamber with a sensitive geometric area of ~500 cm^2 per unit. The gas filling is a mixture of xenon (90%) and methane (10%) at 1.5 bar pressure. The incoming photons are absorbed in the xenon gas by photo-electric absorption and the resulting ionisation cloud is then amplified in an "avalanche" of ionisations by the strong electric field near the microstrip anodes. Significant electric charge is picked up on the strip as an electric impulse. The position of the electron avalanche in the direction perpendicular to the strip pattern is measured from the centroid of the avalanche charge. The orthogonal coordinate of an event is obtained from a set of electrodes deposited on the rear surface.

The X-ray window of the detector is composed of a thin (250 μm) beryllium foil which is impermeable to the detector gas but allows a good transmission of low-energy X-rays.

A collimator structure with square-shaped cells is placed on top of the detector entrance window. It gives support to the window against the internal pressure and, at the same time, limits and defines the field of view of the detector. It has an 85% on-axis transparency. The collimator is important for reducing the count rate caused by the cosmic diffuse X-ray background. However, the presence of the collimator also means that sources near the edge of the field of view will be attenuated with respect to on-axis sources (see Fig. 2). The materials for the collimator (molybdenum, copper, aluminium) have been selected in order to minimise the detector background caused by K fluorescence.

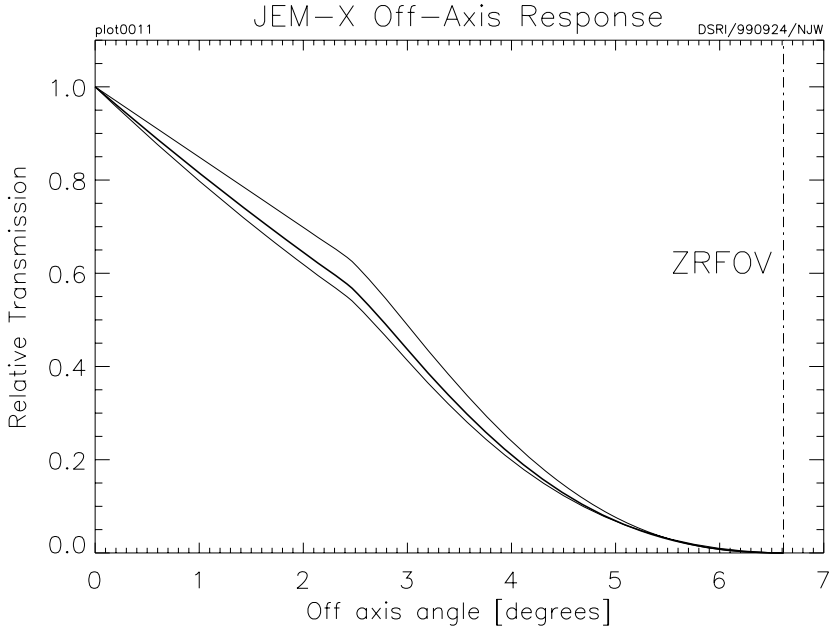

Figure 2: Off-axis response of JEM-X below 50 keV. The middle curve shows the average transmission through the collimator including all azimuth angles.

Four radioactive sources are embedded in each detector collimator in order to calibrate the energy response of the JEM-X detectors in orbit. Each source illuminates a well defined spot on the microstrip plate. The gain of the detector gas is monitored continuously with the help of these sources. Figure 3 shows the collimator layout and the locations of the calibration sources.

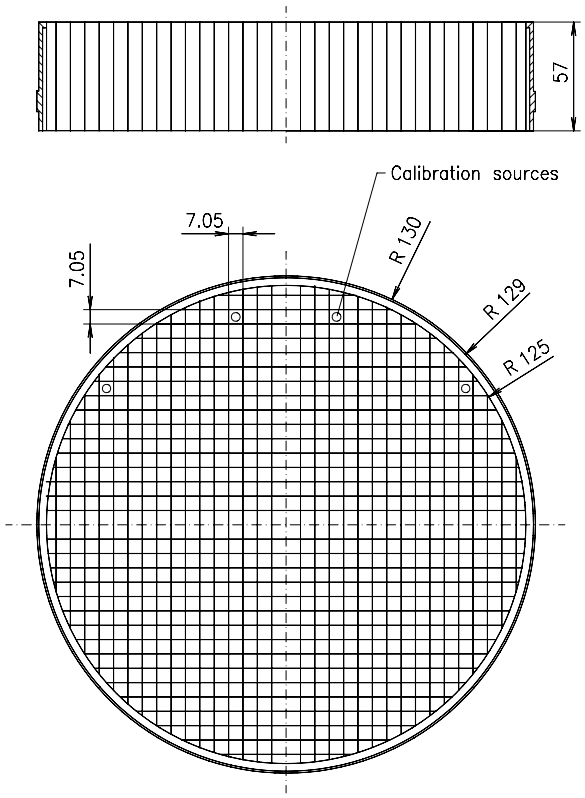

Figure 3: Collimator layout. In this diagram the 4 calibration sources are situated on the upper side. The dimensions are in mm, i.e. collimator height = 57 mm, radius = 130 mm

2.3 The coded mask

The mask is based on a Hexagonal Uniformly Redundant Array (HURA). For JEM-X a pattern composed of 22501 elements with only 25% open area has been chosen. The 25% transparency mask actually achieves better sensitivity than a 50% mask, particularly in complex fields with many sources, or in fields where weak sources should be studied in the presence of a strong source. A mask with lower transparency also has the advantage of reducing the number of events to be transmitted, while at the same time increasing the information content of the remaining events. Considering the

telemetry allocation to JEM-X, this means an improved overall performance for the instrument, particularly for observations in the plane of the Galaxy.

The JEM-X imaging is affected by some (limited) coding noise, but does not suffer from "ghost" images, except in rare cases, because the pattern of the mask only repeats itself near the edges of the mask.

The mask height above the detector (~3.4 m) and the hexagonal mask element dimension (3.3 mm centre-to-centre) define together the angular resolution of the instrument, in this case 3′. Figure 4 illustrates the JEM-X coded mask pattern.

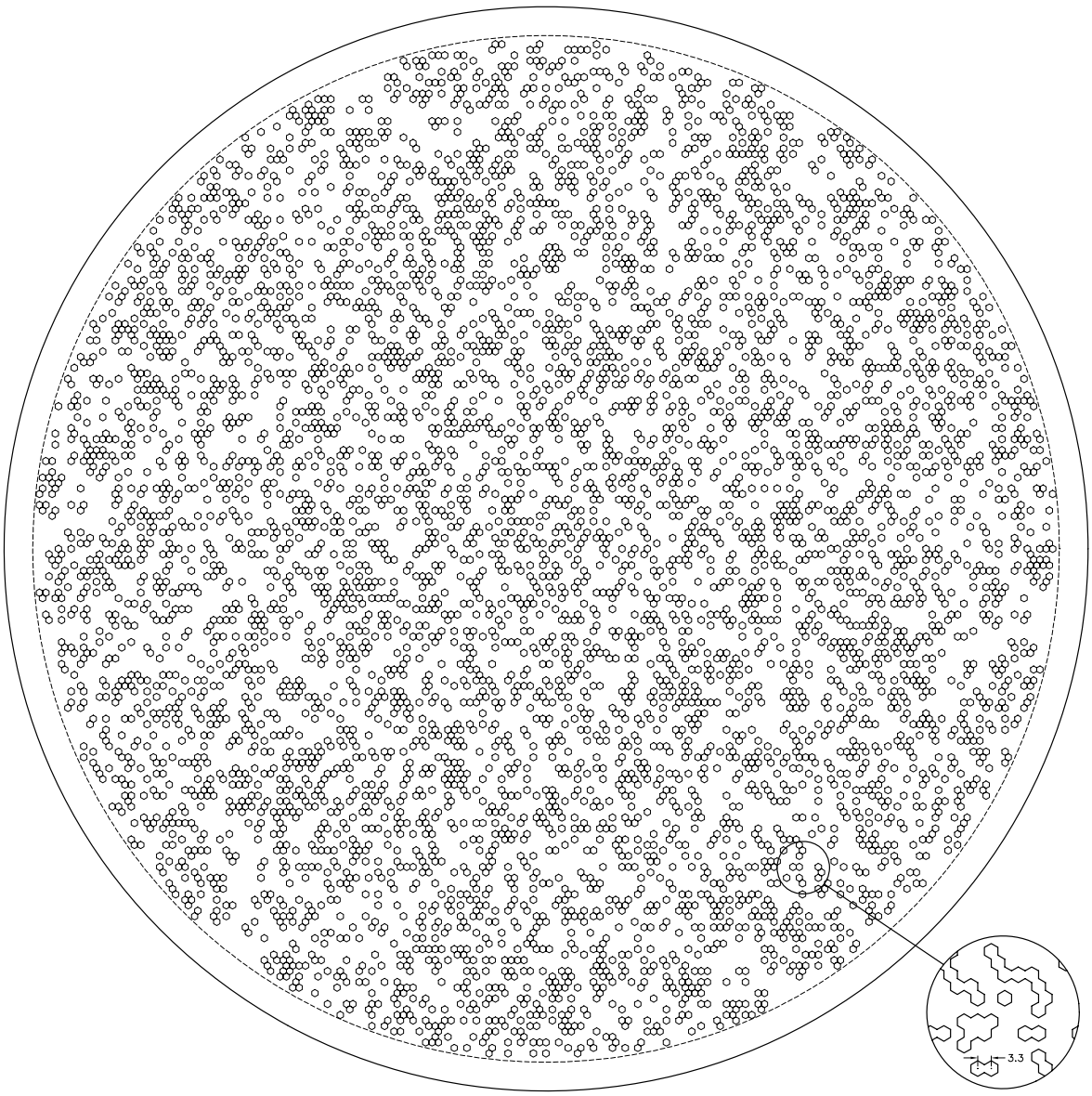

Figure 4: Illustration of the JEM-X coded mask pattern layout without the mechanical interface. The diameter of the coded mask is 535 mm. The mask has a transparency of 25%.

3 Instrument operations

3.1 Telemetry formats and their use

In order to make the best of a situation with a limited telemetry band-width, two types of on-board data reduction can in principle take place for the JEM-X instruments:

1) A grey filter can randomly remove *some of the events* from the telemetry data stream. This takes place automatically when the telemetry buffer fills up beyond a certain limit and will typically happen for JEM-X count rates higher than about 70 cts/s including background, or ~600 mCrab.
2) The on-board software can switch to a "reduced event" telemetry format which removes *part of the information* about each event from the telemetry data stream. For each observation, two formats, "primary" and "secondary" can be defined. Observations will begin in the "primary" format and can switch to the "secondary", if the current countrate is too high – and switch back if the possibly higher transmission rate is no longer required.

In practice, all data formats except for the "Full Imaging" default format suffer various shortcomings – e.g., lack of spatial gain corrections due to lacking position data or very limited support within the OSA software – that make them of little use to general observers. Therefore, the telemetry format can not be chosen by the user in PGT, but is pre-set to "Full Imaging" for primary and secondary format on-board.

In the unlikely case that a specific observation requires the use of another telemetry format than Full Imaging, the observer needs to specify and justify this fact in the scientific justification. If accepted, ISOC would then set the required modes before scheduling the proposal.

3.2 The grey-filter mechanism

The grey-filter process can operate with 32 different transmission fractions. These fractions are T= 1/32, 2/32, …, 31/32, 32/32. The filter values to be used will be chosen by the instrument electronics during the actual observation, taking into account the total background count rates. The grey filter will always be adjusted automatically by the on-board software to match the data stream to the available telemetry capacity, thus the term "automatic grey filter". Whenever the grey filter level is changed (decrease or increase) the on-board software checks whether a telemetry format change should also take place – in the default set-up (see above) this has no effect, as the Full Imaging format is used throughout.

3.3 TM buffer flushing

The JEM-X instruments have an internal buffer capable of storing up to 60000 events. This allows JEM-X to accommodate temporary count rate increases without data loss. But if the telemetry allocation averaged over a science window does not allow transmitting all events then those events which remain in the on-board buffer when a new observation starts will be flushed and lost.

3.4 Detailed overview of the telemetry formats

The following information is given for reference only as the Full Imaging format is the only format that has been calibrated and fully supported by the analysis software.

Table 2: Characteristics of the JEM-X Telemetry Formats.

Format Name	Detector Image Resolution (pixels)	Timing Resolution	Number of Spectral Channels	Event rate (cps) until onset of grey filter
Full Imaging	**256 x 256**	**1/8192s = 122μs**	**256**	**70**
Restricted Imaging	*256 x 256*	*1/8 s = 125 ms*	*8*	*270*
Spectral Timing	*None*	*1/8192s = 122μs*	*256*	*180*
Timing	*None*	*1/8192s = 122μs*	*None*	*500*
Spectrum	*None*	*1/8s = 125 ms*	*64*	*2000*

4 Performance of the instrument

JEM-X is currently operated with one active and one dormant unit. The nominal telemetry allocation is 7 science packets and one housekeeping packet per 8 seconds for the active unit. This allows to transmit about 90 counts/s before events will begin to pile up in the onboard buffer – this will eventually force the grey filter mechanism to set in. (90 counts/s corresponds to about 500 mCrab source counts plus the solar minimum instrumental background). At the beginning of a new pointing (science window) the grey filter is set to full transmission, and therefore, even for higher count rates there will always be a period in the beginning of every pointing where all data are transmitted – the catch is that some of the data taken at the end of the pointing may be lost as the on-board buffers are flushed when the following pointing begins.

4.1 Background

The JEM-X background during solar minimum conditions has been measured from a number of empty field observations. The background rate currently is about 35 counts/s in the 3 to 40 keV range, when the spacecraft is outside the radiation belts. Figure 5 shows a background spectrum from JEM-X1, averaged over 60 empty-field observations in March 2004. The background radiation environment is mainly produced by two components: the diffuse X-ray background and the X- and gamma-radiation induced by cosmic rays. The diffuse X-ray background dominates the background below about 15 keV and the cosmic ray induced background dominates at higher energies. The line at about 30 keV is due to fluorescence photons from the Xenon gas in the volumes surrounding the active detector volume. (It is a useful calibration line and an indicator of the effective resolution of the instrument).

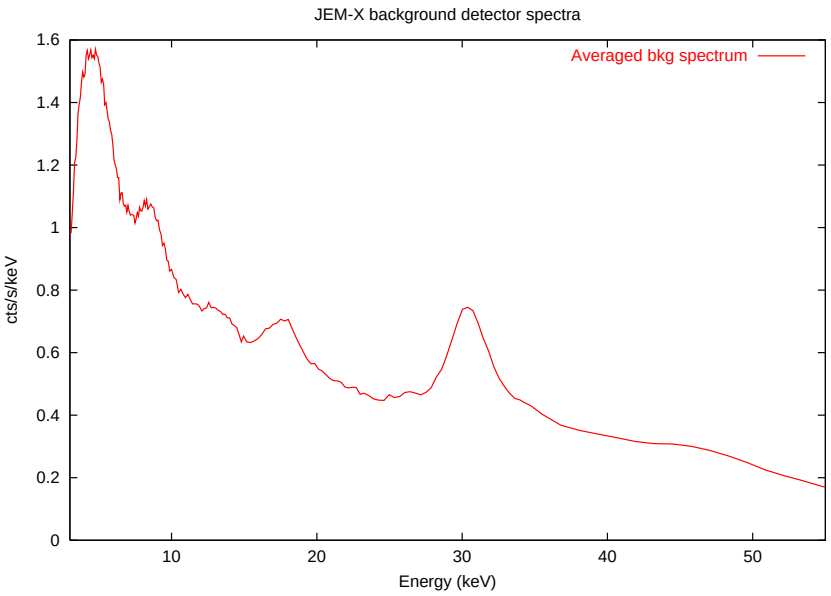

Figure 5: All-detector spectrum of empty field observations showing the combined diffuse and instrumental background.

There are other instrumental lines visible as well. The background increases noticeably at the edge of the detector which is why the useful detector diameter is only 220 mm, rather than the 250 mm physical diameter. (The useful diameter depends on the chosen energy range because the background is strongly energy dependent). The rejection of background events produced by charged particles crossing the detector is accomplished with a combination of pulse height, pulse shape and "footprint"-evaluation techniques. These techniques reach a particle rejection efficiency better than 99.5%.

4.2 Timing stability and resolution

JEM-X observations of the Crab pulsar have shown that the absolute timing is stable to better than 100 μs. The individual JEM-X counts are time binned into bins of width 122 μs. However, the Crab analysis shows that the phase of the timing bins is stable within a few μs.

4.3 Imaging: resolution and detection limits

The accuracy of source position determinations depends on the number of source and background counts and on off-axis angle of the source. Analysis of the standard JEM-X images show that the point spread function of JEM-X is well represented by a symmetrical 2D Gaussian function with a standard deviation of 1.2 arcminutes. This resolution defines the JEM-X ability to check for the presence of multiple sources and also the ability to separate spectra from two sources at small angular separations.

The source positions are best determined when sources are observed on-axis. The JEM-X vignetting function has the shape of a pyramid, so even within the central "fully illuminated" region the instrument response varies significantly between different off axis positions.

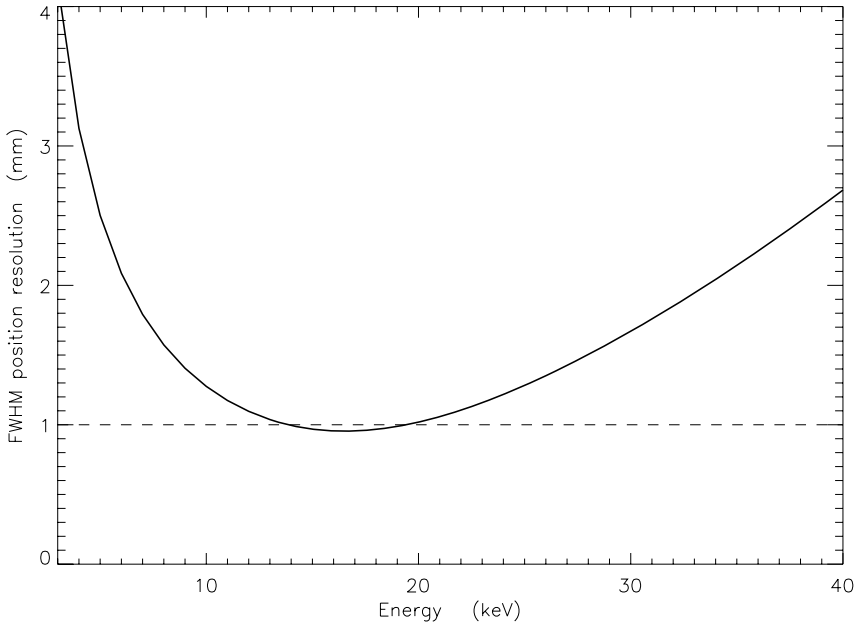

Figure 6: The position resolution in the detector as a function of energy. Note that the positions are rounded to 1mm accuracy in the down-linked data.

The intrinsic detector position resolution is shown as function of energy in Figure 6 for photons entering on-axis. The degradation below 10 keV is caused by the electronic noise of the front-end amplifiers that above 10 keV by the increase of the primary photo-electron range with energy. The intrinsic position resolution of the detector is finer than the pixel size of the coded mask (3.3 mm) over most of the energy range. The determination of the photon positions in the image plane is affected by parallax for higher energy photons entering at off axis angles. This effect is not of prime importance for source positioning, but the smearing of the image affects the off-axis sensitivity at energies above 20 keV.

The alignment of the detector with respect to the INTEGRAL star trackers appear to be stable to better than 10 arcseconds, and the star tracker accuracy is even better than this. The JEM-X OSA 5.1 software has systematic errors of about 30 arcseconds, and therefore does not reproduce the expected accuracy, but work is underway to reduce these systematics.

The source detection limit for single science windows depends on the background conditions and on the off-axis angle of the source, but 20 mCrab sources are reliably detected under normal background conditions if they appear less than 3 degrees off axis. Better sensitivities can be obtained by "mosaicking" overlapping images from several science windows. A deep mosaic image example is shown in Figure 7, while Figure 8 and Figure 9 illustrate the source detection capabilities obtained from mosaic images as function of effective accumulated observation time corrected for dead time, grey filter and vignetting effects.

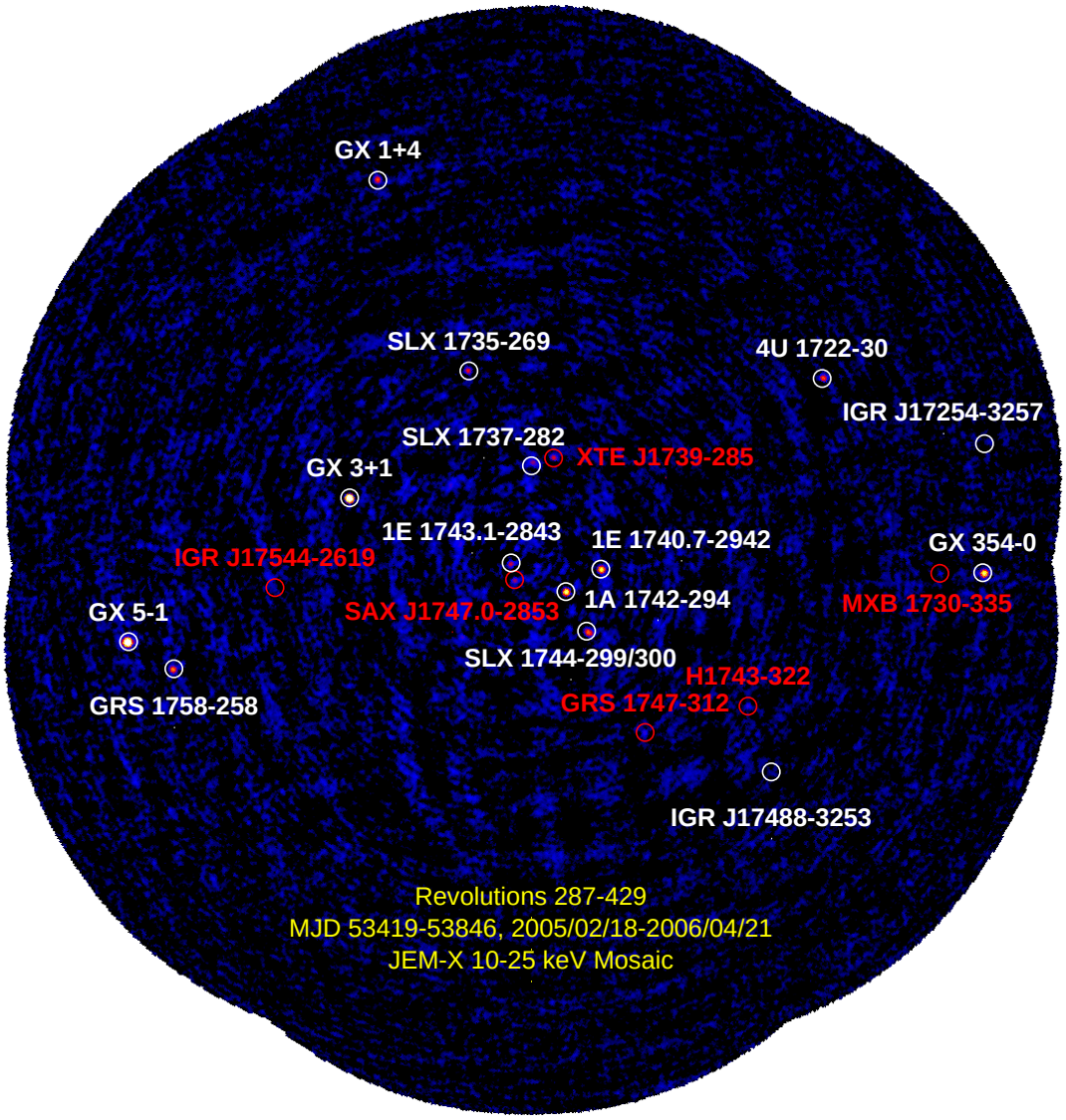

Figure 7: Deep mosaic image of the Galactic Bulge based on the monitoring program of E. Kuulkers et al. The energy range is 10-25 keV and the field ~13 deg wide.

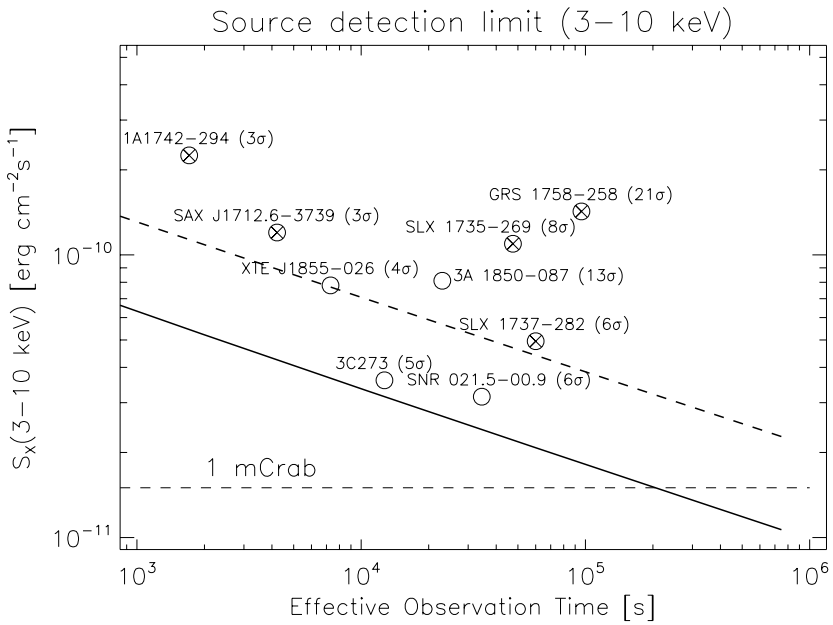

Figure 8: Source detection capabilities in the 3 to 10 keV band as function of effective accumulated observation (exposure) time in JEM-X mosaic images corrected for dead time, grey filter and vignetting effects. The thick solid curve is obtained from simulations where an isolated source must be detected at 6 σ in the deconvolved image. The dashed line represents the case where there are additional sources in the field of view giving a background corresponding to a total of 1 Crab. Examples of actual observations are given: the source 3C 273 and the other empty circles are instances of isolated sources, while the crossed circles represent sources observed in the crowded Galactic Centre region. The σ values given in parentheses are obtained from a measure of the highest source pixel in significance mosaic maps with default pixel size (1.5 arcmin).

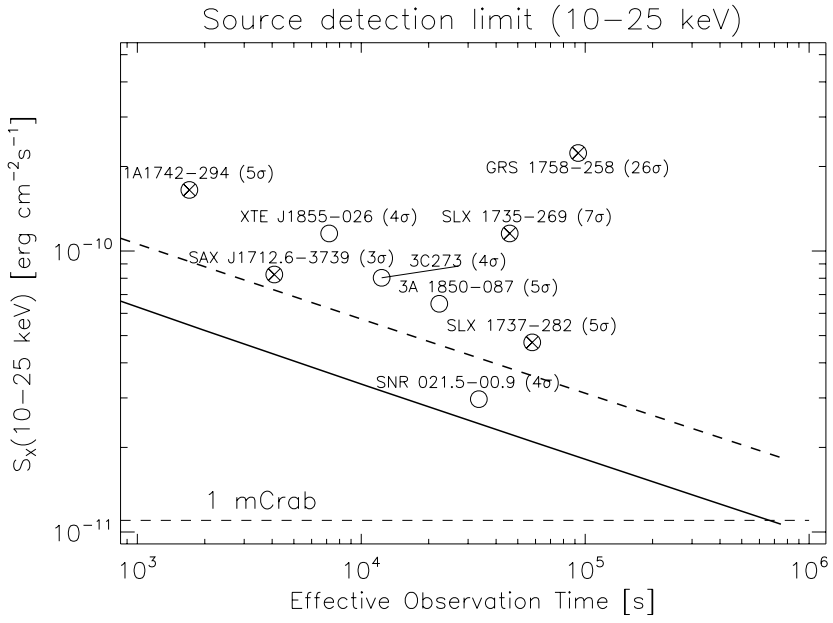

Figure 9: Same as Figure 8 but for the energy range 10 to 25 keV.

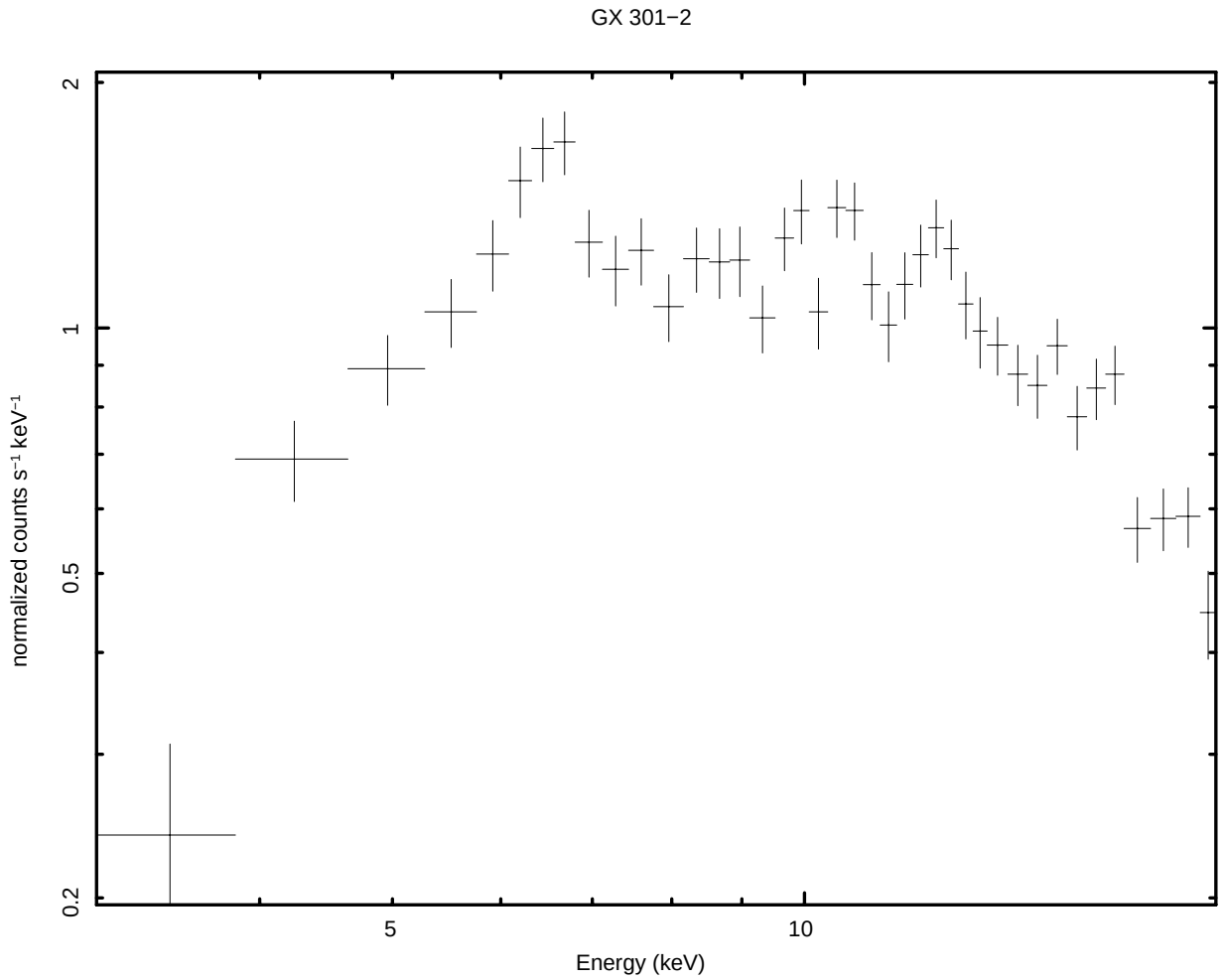

Figure 10: JEM-X spectrum of GX 301-2 obtained from a single pointing of 2500 s. The spectrum can be fitted with an absorbed power law and a Gaussian iron emission line found at ~6.5 keV.

4.4 Spectral analysis

For bright sources spectra can be extracted in a straightforward manner using the spectrum extraction step of the OSA software. An example is given above in Figure 10. This gets more problematic for weak sources in crowded fields, where contamination from the brighter sources affects results. In these cases, extracting spectra from mosaic images is recommended. An example is given in Figure 11 for IGR J17254-325, a source of ~2 mCrab in the 3-10 keV band surrounded by brighter sources.

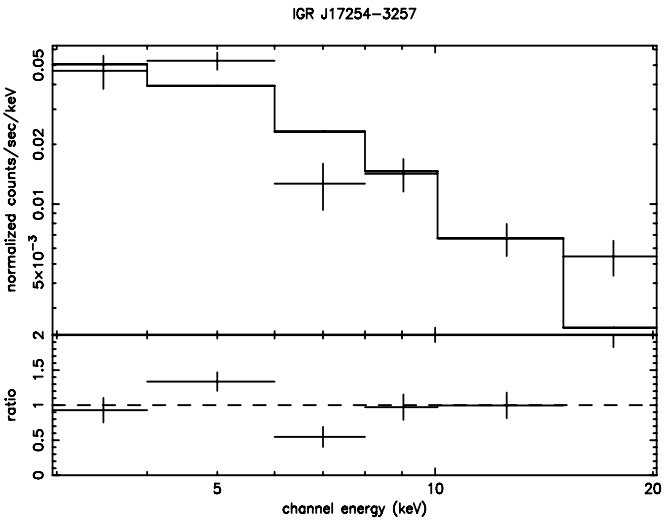

Figure 11: Spectrum of IGR J17254-3257, obtained from mosaic images with ~250 ks total exposure.

4.5 X-ray burst detection

X-ray bursts can be searched for using JEM-X detector light curves with typically ~10 s time bins. In order to verify that a burst found in the detector light curve really comes from a point source an image must be generated corresponding to the time interval of the burst and be compared to a corresponding image covering an equivalent interval before or after the burst. Once a point source origin has been verified the source light curve and spectrum can be extracted and investigated for the burst characteristics. As an example, we present here the detection with JEM-X of the first observed X-ray burst from the source IGR J17254-3257 on February 17, 2004 (Brandt et al., ATel 778).

Figure 12 shows the detector light curve (in black) together with IGR J17254-3257 source light curve (in red) both in the 3-10 keV energy band with 10 s time bins in a 6 minute time interval. One can actually see on the detector light curve another stronger burst from the source 1A 1742-294 occurring less than one minute after the former. The source light curve, which is vignetting corrected, shows that the IGR J17254-3257 burst reaches about 10 times the intensity of the emission outside the burst.

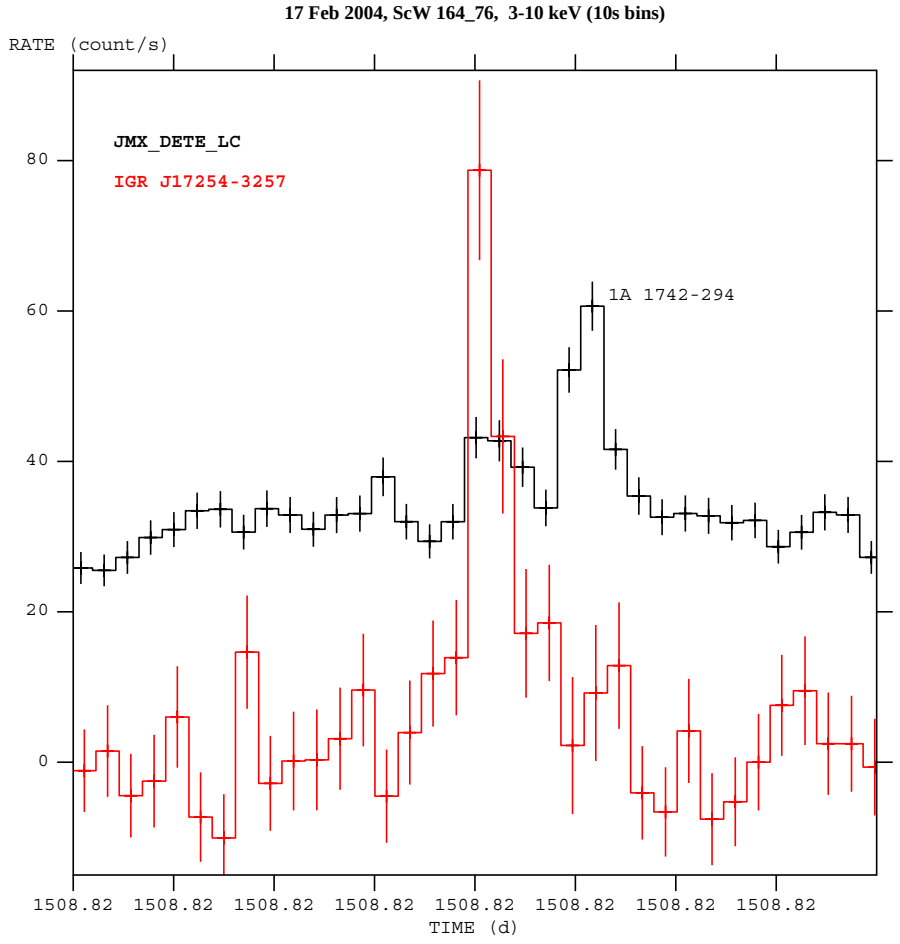

Figure 12: JEM-X detector light curve (black) and IGR J17254-3257 source light curve (red) during a 6 minute interval around the burst that occurred at UTC 19:44:00 on 17 February 2004.

Figure 13 shows the 45 s exposure taken during the burst (left) where only IGR J17254-3257 is visible and the whole science window exposure (right) where a number of other sources are also visible, but not IGR J17254-3257 due to its very low persistent emission. A zoom around the position of IGR J17254-3257 is also displayed in each case.

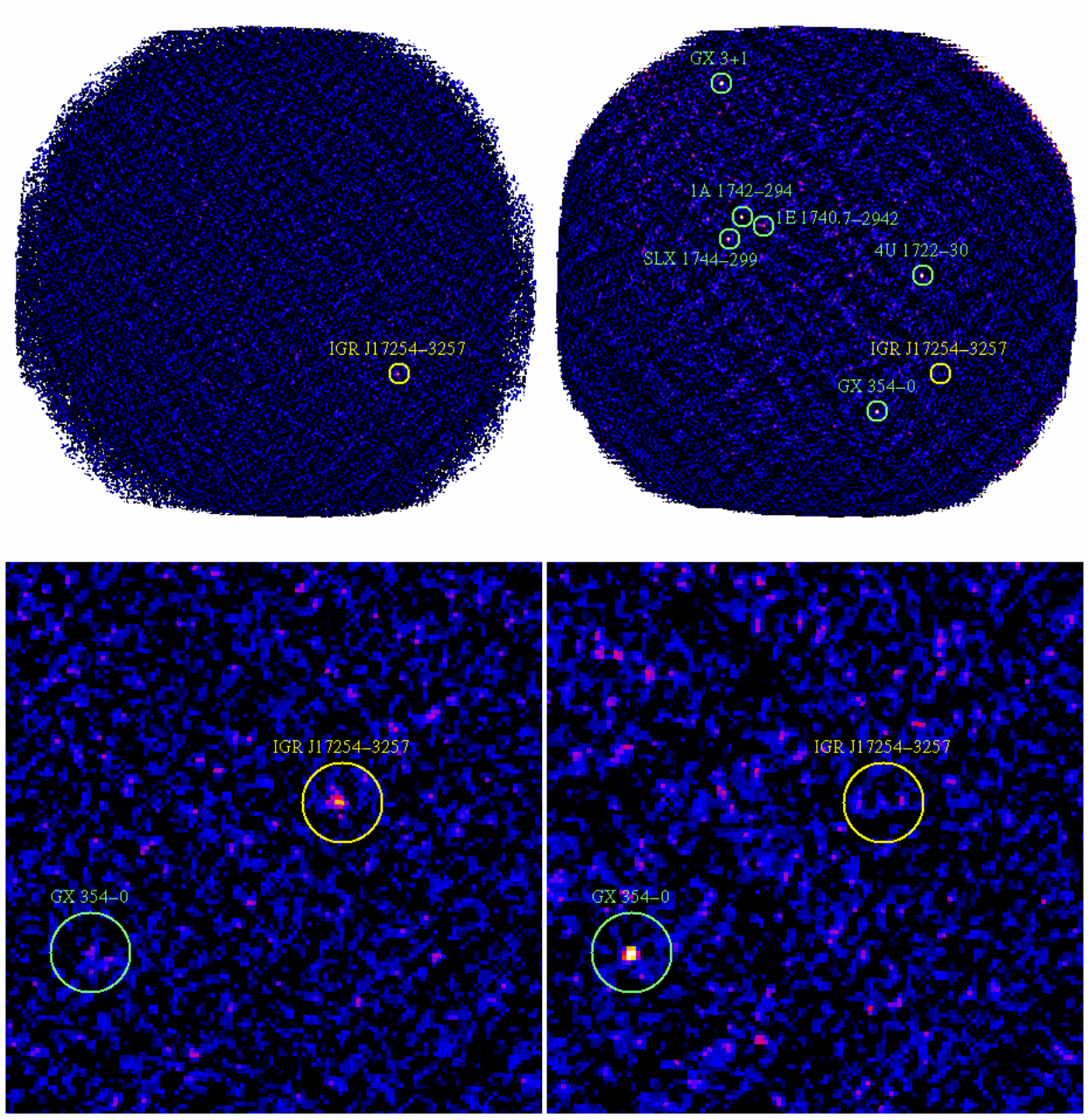

Figure 13: JEM-X 3-10 keV images obtained during a 45 s exposure around the X-ray burst from IGR J17254-3257 (left) and over the whole science window 01640076 (right).

4.6 Detector energy resolution

The energy resolution of the JEM-X instruments slowly degrades with time when the instruments are used. This is the primary reason why only one JEM-X unit is used at a time. Two effects have been noted to change over time: one is an increase in the recovery time for local modifications (drops) in the gas amplification following large charge deposits on the microstrip plate caused by the passage of heavy cosmic rays. The second effect is a gradual change (increase) of the gas amplification for a constant detector voltage. This change is not the same everywhere on the detector, and requires remapping the gain map using the xenon fluorescence line from time to time. Physically, the degradation is suspected to be caused by gradual changes in the conductivity of the microstrip glass substrate due to ion migration. The JEM-X team generates regular updates to the response files to be used with the OSA, in order to respond to this evolution.

The degradation of the energy resolution is most noticeable at the highest energies. It can be described by an additional, slowly time-varying, term in the equation below

$$\Delta E/E = 0.4 \times [(1/E[keV]) + (1/(Enoise)[keV])]^{1/2}$$

E_{noise} can be interpreted as that energy where the resolution has degraded by a factor sqrt(2). For JEM-X 1, after two years of use, E_{noise} is close to 40 keV.

4.7 Sensitivity for line detection

Figure 14 and Figure 15 show the detection limits for narrow lines at 6 keV (close to the Iron K line complex) and at 20 keV as well as the loci for 0.001, 0.1 and 1 keV Equivalent Width (EW).

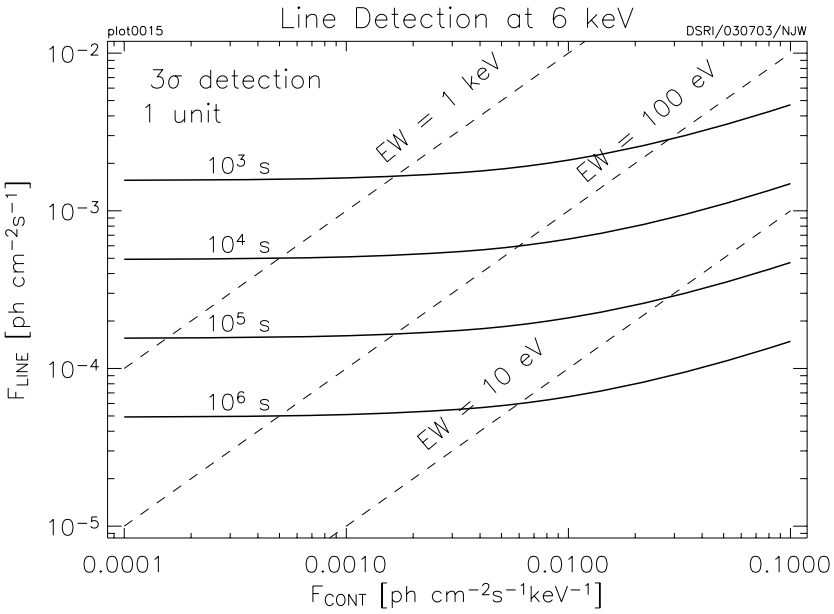

Figure 14: The 3σ line detection limits at 6 keV as a function of the continuum flux at 6 keV, for a single JEM-X unit. The dashed lines represent constant Equivalent Width (EW).

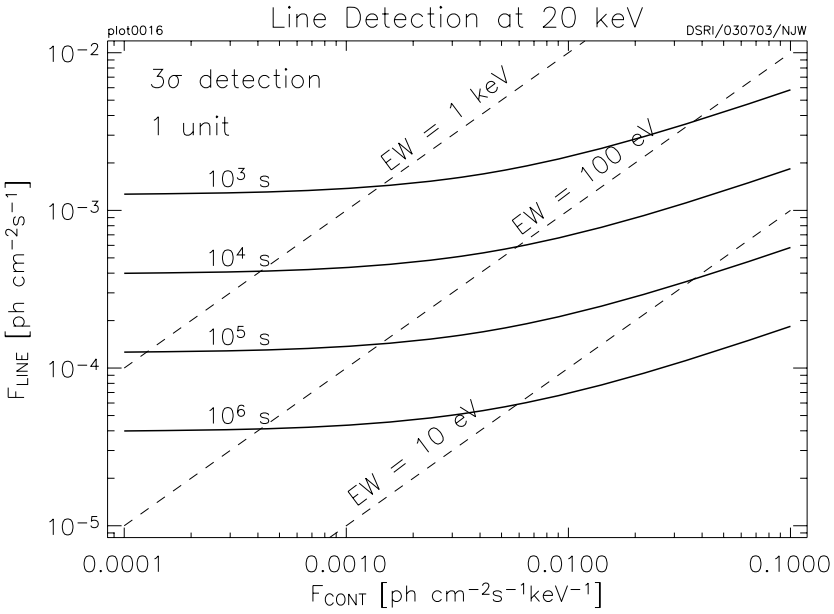

Figure 15: The 3σ line detection limits at 20 keV as a function of the continuum flux at 20 keV, for a single JEM-X unit. The dashed lines represent constant Equivalent Width (EW).

5 Observation "cook book"

5.1 Considerations of the use of the instrument

The primary role of JEM-X is to provide data on the X-ray flux and variability of the targets observed by the two main gamma-ray instruments IBIS and SPI. JEM-X can often pinpoint the source positions with a better precision than IBIS and is thus capable of contributing to the identification of new sources.

The sensitivity of a coded mask instrument like JEM-X is critically dependent on the software used to analyse the data - much more so than for simpler types of X-ray instruments. The sensitivity examples mentioned below should therefore not be considered as final. Improvements in the spectrum extraction software are expected which may increase the S/N. Likewise, specific user choices during the data analysis can reduce the effective area to be used for a given JEM-X data set. This can lead to the necessity of using constant offsets when doing simultaneous spectral fitting of JEM-X spectra together with other Integral spectra.

Users should also be aware that the current spectral extraction and vignetting corrections for sources with off-axis angles greater than 3 or 4 degrees should be interpreted with caution.

Concerning the source detectability, it can be noted that during the Galactic Plane Scan observations (2200 s each) sources down to 20 mCrab are reliably detected when they are inside the central 10° of the field of view. In the same observations many weaker sources – down to 3 mCrab – are also found if they are within the central few degrees of the field of view. These numbers refer to observations with a single JEM-X unit.

5.2 Loss of JEM-X sensitivity due to dithering

Most INTEGRAL observations are done using a 5x5 dither pattern with points spaced 2.17° apart. Dithering is necessary for SPI and recommended for IBIS. Unfortunately, such dithering does not allow JEM-X to observe the target source continuously. In the 5x5 mode, only the central 9 out of the 25 dither pointings yield useful JEM-X spectral data for the central source. The target is simply too far off axis during the remaining 16 dither (see also , p. 8). Table 5 shows the average degradation for the different spacecraft dithering patterns.

Table 3: Effective JEM-X observation times for different dithering modes.

Dithering mode	Effective observation time
Staring	100%
Hexagonal dither	69%
''5 × 5'' dither	23%

5.3 How to estimate observing times

This section describes how to estimate observing times in order to detect X-ray continuum emission and line emission with JEM-X. It is assumed that there is *no dithering* (i.e. STARING mode) and that only one JEM-X unit is used. The instrument sensitivities quoted here are basically the same as in AO-3.

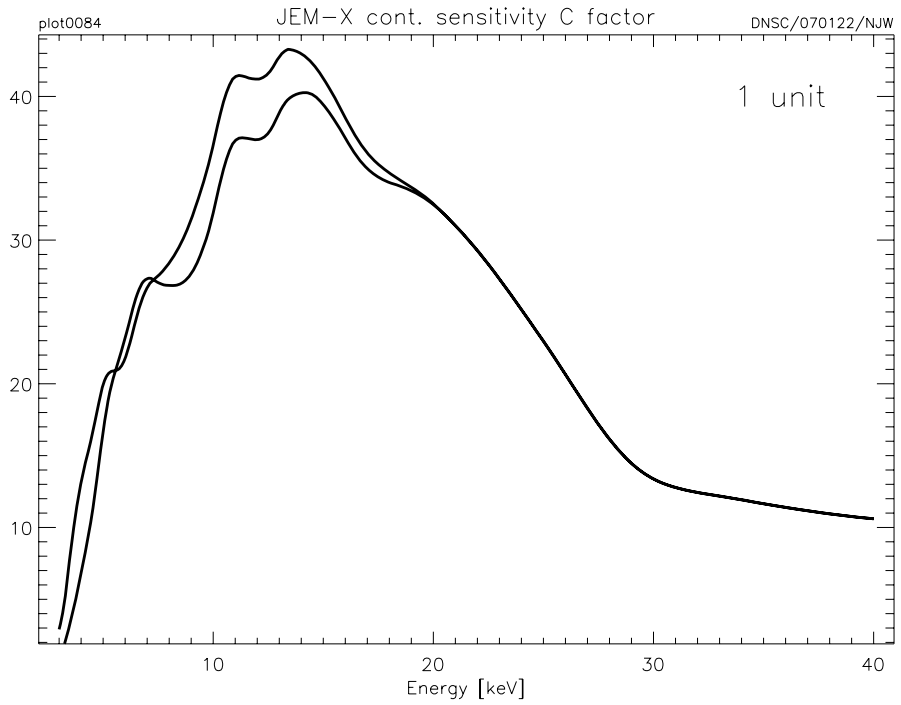

Figure 16: C-factor for estimating the continuum sensitivity for a single JEM-X unit. The upper curve applies to a situation where the gain is high and the lower curve to where it is low.

5.4 Continuum emission

Figure 16 gives a plot of the factor *C(E)* to be used together with the following equation in order to estimate the continuum sensitivity for various detection levels (N_σ = number of sigmas) and observation times t_{obs} (s). $F_{cont}(E)$ is the continuum flux (photons cm^{-2} s^{-1} keV^{-1}) and ΔE the energy resolution (keV):

$$N_\sigma = F_{cont}(E) \times \sqrt{\Delta E \times t_{obs}} \times C(E)$$

5.5 Practical examples

This section gives some practical examples which illustrate the use the formulae described in the previous section. To conclude, Table 5 lists the actual JEM-X background count rates for a single JEM-X unit as well as the observed count rates for the Crab (Nebula and pulsar) on-axis, as measured in-orbit.

5.5.1 Spectroscopy and continuum studies

Consider a 1 mCrab† AGN with a photon spectral index of 1.7 when compared in the 3-10 keV band. How much observation time is needed to do spectroscopy?

Assume a staring observation i.e. no sensitivity loss due to dithering and a requirement to have a 5sigma measurement in a bandwidth equal to the FWHM detector resolution.

Table 4 shows the result at three selected energies.

Table 4: JEM-X spectroscopy

E(keV)	ΔE(keV)	Flux (photons $cm^{-2}s^{-1}keV^{-1}$)	C(E)	Required Observation Time (ks)
4	0.9	5.0×10^{-4}	10	1300
10	1.5	1.1×10^{-4}	34	1500
20	2.1	3.3×10^{-5}	33	12000

† The somewhat imprecise unit is here taken to use the source flux integrated over the energy interval from 3 to 10 keV relative to the Crab flux integrated over the same interval.

5.5.2 Comparing 5x5 dither and hexagonal dither

The usual observation mode of INTEGRAL is shifting the boresight in a dither pattern, most often a 5x5 pattern with a step size of 2.17 deg. A hexagonal pattern (7 pointings) with an offset of 2.0 deg is also an option.

Figure 2 (p. 8) shows the throughput fraction as a function of off-axis angle and the right hand side of the expression for N_σ in section 5.4 must be expanded to include this fraction as a factor as well.

Take an observation of a 30 mCrab source in a 5x5 dither where the total observation time is 90 ks (an hour per pointing), as given in the table on the right. The combination of these observations gives $N_\sigma = 14.8$. If the same observation time is spent in a hexagonal dither then the numbers come out as given in the lower part of the table and the combined observations yield $N_\sigma = 27.2$.

90 ks 5x5 dither pattern		
Off-axis (deg)	Time (ks)	N_σ
0.00	3.6	8.1
2.17	14.4	9.6
3.07	14.4	6.7
4.34	14.4	1.7
4.85	28.8	1.0
6.14	14.4	0.0
90 ks hexagonal pattern		
0.00	12.9	15.3
2.00	77.1	23.2

5.5.3 In-orbit count rates for the Crab and the JEM-X background

Table 5: Count rates for a single JEM-X unit (Crab on-axis).

Interval [keV]	**Crab counts s^{-1}**	**Diffuse X-ray Background counts s^{-1}**	**Cosmic Ray induced counts s^{-1}**	**Total bkg counts s^{-1}**
3 - 10	83	2.7	5.0	7.7
10 - 20	27	1.7	5.4	7.1
20 - 35	5.4	0.5	8.5	8.9
Total: 3 - 35	115	4.9	18.8	23.7